

Phase transitions in higher derivative gravity and gauge theory: R-charged black holes

Tanay K. Dey^{*1}, Sudipta Mukherji^{*2}, Subir Mukhopadhyay^{*+3} and Swarnendu Sarkar^{*4}

**Institute of Physics,
Bhubaneswar 751 005, INDIA*

*+Institute for Studies in Theoretical Physics and Mathematics (IPM),
P.O.Box 19395-5531, Tehran, IRAN*

ABSTRACT

This is a continuation of our earlier work where we constructed a phenomenologically motivated effective action of the boundary gauge theory at finite temperature and finite gauge coupling on $S^3 \times S^1$. In this paper, we argue that this effective action qualitatively reproduces the gauge theory representing various bulk phases of R-charged black hole with Gauss-Bonnet correction. We analyze the system both in canonical and grand canonical ensemble.

June 2007

¹e-mail: tanay@iopb.res.in

²e-mail: mukherji@iopb.res.in

³e-mail: subir@iopb.res.in

⁴e-mail: swarnen@iopb.res.in

1 Introduction and Summary

In a recent paper [1], we initiated a study of the phase structure of gravity in anti-de Sitter space in presence of higher derivative corrections. Our motivation stemmed from the fact that due to AdS/CFT correspondence [2,3] a quantum theory of gravity provides natural arena for addressing issues in gauge theory and vice versa. Though absence of a formulation of string theory on AdS space and lack of adequate techniques to study strong coupling regimes of gauge theories make a quantitative comparison difficult, nevertheless, encouraging agreements among qualitative features have been gathered over the last few years. One of the remarkable steps [4] in this realm is the identification of the crossover from the thermal AdS phase to black hole phase, namely the Hawking-Page transition [5], on the gravity side with large N deconfinement transition on the gauge theory side ⁵. Based on this identification, recently, a phenomenological matrix model was proposed [11], which belongs to the same universality class of $\mathcal{N}=4$ supersymmetric $SU(N)$ gauge theory on S^3 at the limit of infinite 't Hooft coupling (λ). This model, which we will call (a, b) -model in the sequel, was characterized by two coefficients a and b which depend on temperature T (and λ). It correctly reproduced the qualitative features of the phase structure of the dual theory on the gravity side. This model was also used to study the transition between AdS soliton and black hole [12]

Following this line of works, in [1] we considered the response of the Hawking-Page transition and the associated thermodynamic phase structure to higher derivative terms in the gravity theory, which appears as α' corrections of the underlying string theory. While a study with general class of higher derivative terms would be desirable, in [1], we restricted ourselves to the Gauss-Bonnet (GB) terms only. The reason for this is that the GB terms can capture non-trivial first order effects of α' correction while admitting explicit black hole solutions [13–19, 29] ⁶. It turned out that the

⁵In many papers, it was argued that this large N transition might even occur at zero coupling [6, 7] and it turned out that for zero coupling, the transition appeared exactly at the Hagedorn temperature of the low temperature thermal AdS phase. As the coupling is increased the Hagedorn and the deconfinement transitions separate out. The Hagedorn transition occurs at a higher temperature than that of the deconfinement transition. However it is also believed that this Hagedorn transition at weak coupling manifests as the deconfinement or Hawking-Page transition at strong coupling. For a related work see [8]. Non-perturbative effects near Hagedorn transition was studied in [9] (see also [10])

⁶GB term is expected to occur only in Heterotic or K3 compactification of type IIA theory but not in type II theories with maximally supersymmetric compactification. The lowest correction in type IIB theory on AdS_5 is of order α'^3 . The thermodynamic phases of the perturbative supergravity solutions as well as their boundary duals have been studied by various authors [21–24]. However the

phase structure in GB theory depends crucially on the GB coupling. For sufficiently strong coupling there is a single big black hole phase which serves as a local minimum below a critical temperature. As the coupling reduces below a critical value, two additional black holes of intermediate and small sizes appear, of which, the former one has negative specific heat while the small hole has positive specific heat. The latter one is stable and corresponds to a local minimum up to a critical temperature beyond which it ceases to exist. From the associated phase diagram, we find that the phase structure is similar to that of a Van der Waals gas. Along with the standard HP transition between the big black hole and thermal AdS, we identified one more phase transition where crossover of the energies of small black hole and big black hole occurs.

A similar study of the various phases in the dual theory is also carried out in [1]. Usually, to describe gauge theory on $S^3 \times S^1$ at zero coupling one writes down an effective action with vev of Polyakov loop on S^1 as the only light degree of freedom. Since it is hard to compute such an action at finite YM coupling, one relies on phenomenological model [11], that belongs to the same universality class of the gauge theory as described in [11]. Appealing to the universal nature of this model near the critical temperature, we analyzed in [1] the $\frac{1}{\lambda}$ dependence of the coefficients (a, b) by mapping the GB corrections to the gauge theory. We also suggest [1] a modified matrix model which, with appropriate restriction on the coefficients of the model, qualitatively captures the bulk properties with α' corrections. This is an extension of (a, b) -model and includes higher power of density of eigenvalues of the vev of Polyakov loop indicating, perhaps, that other operators in matrix model become relevant.

In this paper, we extend our study of the effects of higher curvature corrections to charged sector in the AdS/CFT set up with an aim to identify some universal features of the boundary matrix models at strong coupling. The charged sector of the GB action contains a Maxwell term besides the GB corrections. Maxwell term typically comes in type IIB theory on $AdS_5 \times S^5$ from angular momentum along S^5 direction, or in other words, from the $SO(6)$ gauge symmetry arising from the group of isometries of S^5 . We focus our attention to those black hole configurations which have equal $U(1)$ charges for all the three commuting $U(1)$ subgroups of $SO(6)$. These black holes and their phase structures were considered in [25, 26] (see also [27]). We study the changes of phase structures due to GB corrections in canonical and grand canonical ensembles. On the gauge theory side ⁷, in order to describe the charged

qualitative phase structures in this case is quite similar to that of gravity with GB (α') correction.

⁷We would like to emphasise that the inclusion of GB correction takes us away from type IIB

sector, we use the same model as in [1] except we allow the coefficients of the model to depend on appropriate parameters of the ensemble as well along with the temperature (T) and the t'Hooft coupling (λ). In the following we summarize our results along with some already known facts about phase diagram in absence of GB coupling.

Grand canonical Ensemble (Fixed Potential):

In the grand canonical ensemble, the black hole is allowed to emit and absorb charged particles keeping the potential fixed till the thermal equilibrium is reached, which, in this case, is governed by a fixed chemical potential. Here the phase diagram is characterized by the chemical potential Φ and the GB coupling which we call $\bar{\alpha}$ in the paper.

($\Phi \neq 0, \bar{\alpha} = 0$) : On the gravity side, the phase diagrams have been analyzed in [25, 26]. If the potential Φ is below a critical value, various phases are similar to that of AdS-Schwarzschild black hole while for Φ large enough, the black hole free energy becomes negative compared to that of the thermal AdS at any fixed temperature. On the gauge theory side, at zero and small λ , the phase structure was analysed in [28, 29], while for large λ , a phenomenologically motivated matrix model can be constructed and we will have occasion to elaborate on it at a later stage of this paper.

($\Phi \neq 0, \bar{\alpha} \neq 0$) : This case is studied in section (2.1) where we find the critical value of Φ depends on α . For small Φ , there are three different black hole phases; one of them being unstable. Identifying the rest two as a small and a big black hole, we find that there is a first order phase transition from the small to the big black hole. However, once thermal AdS is included in the phase diagram, we find both the small and big black hole phases are metastable at low temperature and big black hole becomes stable only at high temperature. In order to clearly illustrate the various phases in this range of Φ we construct a Landau function with black hole horizon radius as the order parameter. When Φ is above the critical value, phase diagram shows a single black hole phase which is stable beyond certain temperature while a crossover from black hole phase to thermal AdS occurs for temperature lower than that. If we increase Φ even further, the black hole phase is always found to be stable. All these phases can be summarized in a $(\Phi^2 - \bar{\alpha})$ diagram; see Figure 1. We also note that, in all the above cases, wherever there is Hawking-Page transition from AdS to the black hole phase, the transition temperature is found to decrease with $\bar{\alpha}$.

We study the grand canonical ensemble of the dual theory in section (3.3) and framework. However we will assume that a version of gauge/gravity will continue to hold.

(3.4). Here the parameters of the matrix model depend on the chemical potential (μ). We find for the chemical potential less than the critical value the analysis is similar to that of [1]. As in [1], the matrix model has an extra saddle point that has no analogue in supergravity. We interpret this saddle point with some phase in string theory⁸ Beyond the critical potential we encounter different possible situations depending on the position (expectation value of the Polyakov loop) of the extra saddle point.

Canonical ensemble (Fixed Charge):

In the canonical ensemble, the black hole is allowed to emit and absorb radiation, keeping the charge fixed till the thermal equilibrium is reached and the phase diagrams are characterized by the charge of the black hole, q and the GB coupling $\bar{\alpha}$.

($q \neq 0, \bar{\alpha} = 0$) : The phase structure is discussed in [25, 26] in great detail. There exists a critical charge q_c above which, at all temperature, only one black hole phase exists. Below q_c , there can be at most three black hole phases. We call them small, intermediate and large. While the intermediate one is unstable, the small and big black holes are stable. It was also noted that thermal AdS is not an admissible phase. When we increase the temperature, there is a crossover from a small black hole to a large black hole phase via a first order phase transition.

($q \neq 0, \bar{\alpha} \neq 0$) : This part of the analysis is given in section 2.2, where, we find the phase structure depends on two parameters q and $\bar{\alpha}$. In particular, in $(q^2 - \bar{\alpha})$ plane, we identify two distinct regions (see Figure 5) where region I consists of three black hole phases, while in region II, only one black hole phase exists. Thermal AdS continues to be non-admissible phase. As before, there is a transition from small to big black hole at a critical temperature. This temperature decreases as we increase $\bar{\alpha}$.

Study of the canonical ensemble of the dual theory is discussed in section (3.5). Since the explicit dependence of the coefficients of the matrix model on the chemical potential is very hard to determine at strong coupling, we assume the the zero coupling result is valid there or at least the universality class of the theory does not change once we tune up the gauge coupling. We find that this dependence is consistent with one of the possible scenarios. For this scenario, we write down the matrix model for

⁸This could be related to some state in string theory. At this point it may be mentioned that appearance of string states in boundary theory also occurred in [11, 30] which corresponds to the Gross-Witten transition [31, 32] and which was identified with a crossover from supergravity black hole solution to string state [33].

the fixed charge and find that this model correctly reproduces the phases of the black holes with fixed charge.

The paper is structured as follows. We begin with the thermodynamics of charged sector in presence of GB coupling in section 2. Subsections (2.1) and (2.2) are devoted to discussion of canonical and grand canonical ensembles. The dual theory is discussed in section 3. We begin by reviewing zero charge sector of the dual theory. A short account of the zero and weak 't Hooft coupling results is given in subsection (3.1) and in subsection (3.2) we briefly mention the comparison of phase structures between gravity and matrix model. The rest of the section 3 is devoted to our study of the charged sector. The grand canonical ensemble of the dual theory is considered in subsection (3.3) and (3.4) while the canonical ensemble is discussed in subsection (3.5).

2 Gauss-Bonnet black hole with electric charge

We start with $n + 1$ -dimensional ($n \geq 4$) action

$$I = \int d^{n+1}x \sqrt{-g_{n+1}} \left[\frac{R}{\kappa_{n+1}} - 2\Lambda + \alpha(R^2 - 4R_{ab}R^{ab} + R_{abcd}R^{abcd}) - \frac{F^2}{\kappa_{n+1}} \right]. \quad (1)$$

Here, α is the GB coupling. As the higher derivative corrections are expected to appear from the α' corrections in underlying string theory, we will often refer the GB term as α' correction in this paper. This action possesses black hole solutions which we call charged GB black holes [27]. These solutions have the form

$$ds^2 = -V(r)dt^2 + \frac{dr^2}{V(r)} + r^2 d\Omega_{n-1}^2, \quad (2)$$

where $V(r)$ is given by

$$V(r) = 1 + \frac{r^2}{2\hat{\alpha}} - \frac{r^2}{2\hat{\alpha}} \left[1 - \frac{4\hat{\alpha}}{l^2} + \frac{4\hat{\alpha}m}{r^n} - \frac{4\hat{\alpha}q^2}{r^{2(n-1)}} \right]^{\frac{1}{2}}. \quad (3)$$

In the above, $\hat{\alpha} = (n-2)(n-3)\alpha\kappa_{n+1}$, while l is related to the cosmological constant as $l^2 = -n(n-1)/(2\kappa_{n+1}\Lambda)$. The parameter m is related to the ADM mass of the hole, M as

$$M = \frac{(n-1)\omega_{n-1}m}{\kappa_{n+1}}, \quad (4)$$

where ω_{n-1} is the volume of the unit $(n-1)$ -sphere. The parameter q gives the charge

$$Q = \frac{2\sqrt{2(n-1)(n-2)}\omega_{n-1}q}{\kappa_{n+1}}, \quad (5)$$

of the electric gauge potential

$$A_t = -\sqrt{\frac{n-1}{2(n-2)}} \frac{q}{r^{n-2}} + \Phi, \quad (6)$$

where Φ is a constant which we will fix below. Denoting r_+ as the largest real positive root of $V(r)$, we find that the metric (3) describes a black hole with non-singular horizon if

$$\left(\frac{n}{n-2}\right)r_+^{2n-2} + l^2 r_+^{2n-4} \geq q^2 l^2. \quad (7)$$

Finally, we shall choose the gauge potential A_t to vanish at the horizon. This fixes Φ to be

$$\Phi = \sqrt{\frac{n-1}{2(n-2)}} \frac{q}{r_+^{n-2}}. \quad (8)$$

This quantity is the electrostatic potential between the horizon and infinity. Asymptotically, the metric (3) goes to AdS space, as in this limit,

$$V(r) = 1 + \left[\frac{1}{2\hat{\alpha}} - \frac{1}{2\hat{\alpha}} \left(1 - \frac{4\hat{\alpha}}{l^2}\right)^{\frac{1}{2}} \right] r^2. \quad (9)$$

Hence we notice that the metric is real if,

$$\hat{\alpha} \leq \frac{l^2}{4}. \quad (10)$$

We shall restrict ourselves to $\hat{\alpha}$ which satisfy the above bound. In this paper, we will primarily consider black holes in five dimensions ($n = 4$). However, it is easy to extend the results of this section to higher dimensions.

The thermodynamic properties of the black hole will depend on whether we consider the canonical ensemble (fixed charge Q) or grand canonical ensemble (fixed potential Φ). The equilibrium temperature T can be identified from the period β of the Euclidean time of the metric (3), which in five dimensions is given by

$$\beta = \frac{2\pi r_+(r_+^2 + 2\hat{\alpha})}{r_+^2 + 2r_+^4/l^2 - q^2/r_+^2}. \quad (11)$$

As it will be useful for us to write thermodynamic quantities in terms of dimensionless quantities, we define

$$\bar{r} = \frac{r}{l}, \bar{\alpha} = \frac{\hat{\alpha}}{l^2}, \bar{q} = \frac{q}{l^2}, \bar{m} = \frac{m}{l^2}. \quad (12)$$

In terms of these quantities, (11) can be expressed as

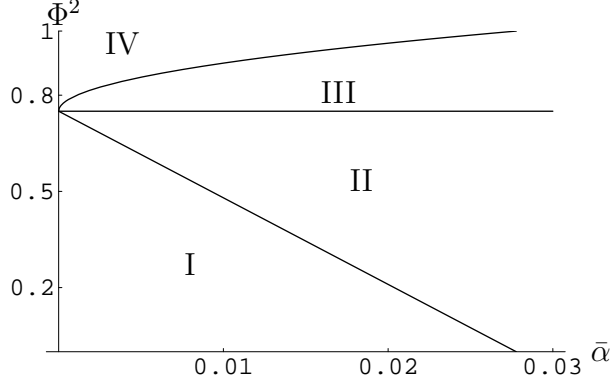


Figure 1: The curves in the $(\bar{\alpha}-\Phi^2)$ plane separating various regions with different behaviours of black holes.

$$\beta = \frac{2\pi l \bar{r}(\bar{r}^2 + 2\bar{\alpha})}{\bar{r}^2 + 2\bar{r}^4 - \bar{q}^2/\bar{r}^2}. \quad (13)$$

2.1 Grand canonical ensemble

In the grand canonical ensemble, with fixed potential Φ , the free energy can be computed from the Euclidean continuation of the action (1). We obtain the action (subtracting the AdS background) as

$$I_{\text{gc}} = -\frac{\omega_3 l^2 \beta}{\kappa_5(\bar{r}^2 + 2\bar{\alpha})} \left[\bar{r}^6 + (18\bar{\alpha} - 1 + 4\Phi^2/3)\bar{r}^4 + 3\bar{\alpha}(1 - 8\Phi^2/3)\bar{r}^2 - 6\bar{\alpha}^2 \right], \quad (14)$$

where β is inverse of T expressed in terms of potential

$$\beta = \frac{2\pi l(\bar{r}^2 + 2\bar{\alpha})}{\bar{r}(1 - 4\Phi^2/3 + 2\bar{r}^2)}. \quad (15)$$

It will be important for us to find out the number of turning points of $\beta(\bar{r})$ as we vary $\bar{\alpha}$ and Φ . First of all, the nature of $\beta(\bar{r})$ depends crucially on the value of Φ^2 . For $\Phi^2 > 3/4$, $\beta(\bar{r})$ blows up at $\bar{r}^2 = (4\Phi^2/3 - 1)/2$. Consequently, the temperature is zero. Following [25, 26], we would like to identify this with an extremal hole. For \bar{r} less than this value, $\beta(\bar{r})$ becomes negative. It can easily be checked that as long as $\Phi^2 > 3/4$, regardless of the value of $\bar{\alpha}$, there is no turning point of $\beta(\bar{r})$. If, on the

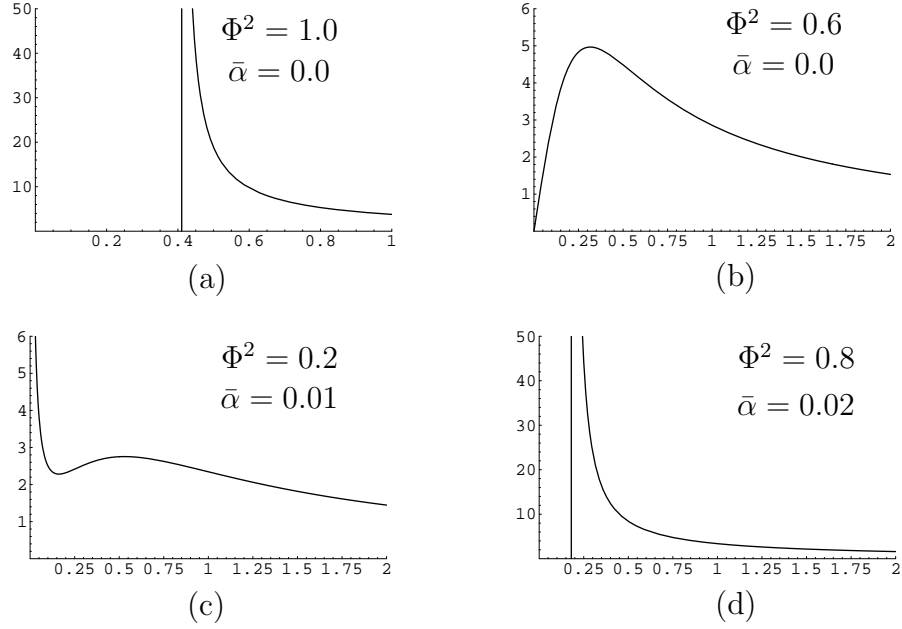


Figure 2: Plots of β vs \bar{r} for various values of $(\Phi^2, \bar{\alpha})$.

other hand, $\Phi^2 = 3/4$, β diverges at $\bar{r} = 0$ and goes to zero for large \bar{r} . Now, to have turning points, $\partial\beta/\partial\bar{r} = 0$. This gives

$$\bar{r}_{1,2}^2 = \frac{1}{12} \left(3 - 36\bar{\alpha} - 4\Phi^2 \pm \sqrt{(-3 + 12\bar{\alpha} + 4\Phi^2)(-3 + 108\bar{\alpha} + 4\Phi^2)} \right). \quad (16)$$

From here, it follows that in order to have real roots, $\bar{\alpha}$ should *not* lie within the window

$$\frac{1}{36} \left(1 - \frac{4\Phi^2}{3} \right) \leq \bar{\alpha} \leq \frac{1}{4} \left(1 - \frac{4\Phi^2}{3} \right). \quad (17)$$

However, it is easy to check that for $\bar{\alpha} \geq \frac{1}{4} \left(1 - \frac{4\Phi^2}{3} \right)$, $\bar{r}_{1,2}^2$ are negative while $\bar{\alpha} \leq \frac{1}{36} \left(1 - \frac{4\Phi^2}{3} \right)$, $\bar{r}_{1,2}^2$ are positive. Hence, we have the following picture. For $\Phi < \sqrt{3}/2$, β has two turning points only if

$$\bar{\alpha} \leq \frac{1}{36} \left(1 - \frac{4\Phi^2}{3} \right). \quad (18)$$

The above features of $\beta(\bar{r})$ can be nicely summarized in a $(\Phi^2 - \bar{\alpha})$ diagram. This is shown in Figure 1. The region satisfying (18) is the region I in the figure. So, here $\beta(\bar{r})$ has two turning points. However, note that for $\Phi^2 < 4/3$ and $\alpha = 0$, $\beta(\bar{r})$ has only one turning point at non-zero \bar{r} . In the rest of the regions namely II, III and IV,

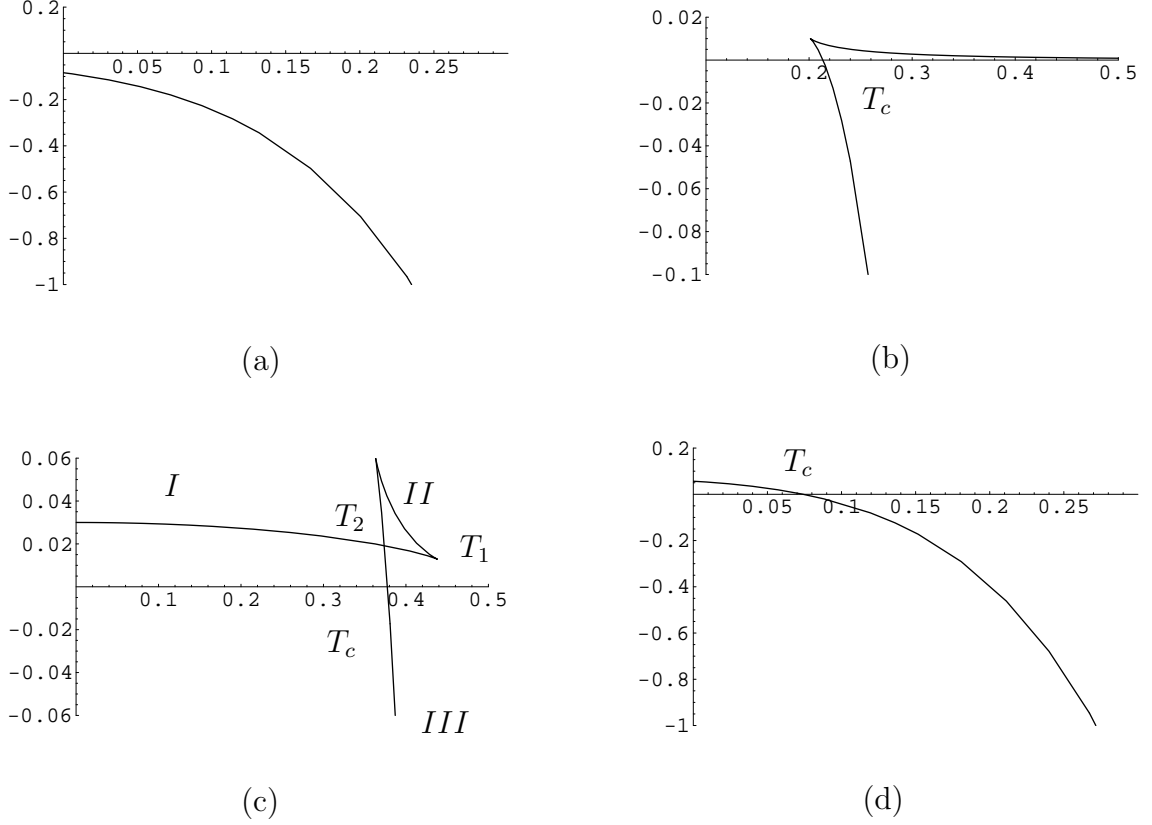


Figure 3: Free energy W as a function of T . (a), (b), (c), (d) correspond to values of Φ^2 and $\bar{\alpha}$ of Figure(2)

there are no turning points of $\beta(\bar{r})$. However, as in I, in region II, $\beta(\bar{r})$ diverges at $\bar{r} = 0$ while in regions III and IV, $\beta(\bar{r})$ blows up at finite non-zero values of \bar{r} . There are other differences in these four regions (particularly when the free energies of the black holes are considered). This is what we discuss in the next paragraph. Various representative plots of the β versus \bar{r} for all these regions are shown in Figure 2.

Free Energy: The free energy can be obtained from (14) as $W = I_{\text{gc}}/\beta$. For different values of the parameters, W has been plotted as a function of temperature in Figure 3. In this figure, (a) corresponds to the parameter values where we have only one stable black hole solution. This is also the situation in the case of (d). However, there is a distinct difference in their phase structures as is evident from the plots. While the black hole phase has lower free energy than thermal AdS in (a) for all temperatures, there is a Hawking-Page transition at T_c in (d). This difference can easily be located

in $(\Phi^2 - \bar{\alpha})$ diagram in Figure 1. In the region IV of this figure, black hole at $T = 0$ has less energy than the thermal AdS and hence is stable. However, in regions II and III, a hole at $T = 0$ is in a metastable phase while AdS is the stable one. Hence this hole would decay to AdS by radiating away its energy. The line separating III and IV represents hole with zero free energy at $T = 0$. The equation of this line as a function of $\bar{\alpha}$ and Φ^2 is obtained by setting $W(\bar{r}, \bar{\alpha}, \Phi^2) = 0$, where $\bar{r}^2 = 1/2(1 - 4\Phi^2/3)$. Note that this also means that on this line the Hawking-Page temperature vanishes.

Now returning back to Figure 3(b), we see that at low temperatures there is no black hole phase. Two black hole phases appear as we increase the temperature. The small one turns out to be unstable and the large one undergoes a Hawking Page transition at T_c . Note that Figure 3(c) is similar to the one we found in our previous paper [1] (i.e for $\Phi^2 = 0, \bar{\alpha} \neq 0$). As in [1], we have therefore the following scenario. At low temperature, free energy has only one branch (branch I). However, as temperature is increased, two new branches (branch II and III) appear. Branch II meets branch I at a certain temperature (T_1) and they both disappear. On the other hand, branch III continues to decrease, cuts branch I at a particular temperature (T_2) and becomes negative at temperature T_c . These three branches represent small, intermediate and large black hole. Out of these three, the intermediate black hole is unstable with negative specific heat, while the rest are classically stable. As in [1], we get two first order phase transitions (HP1, HP2). HP1 is a transition between small and large black hole at temperature T_2 and the other (HP2) is the usual transition between AdS to large black hole as T_c .

It is easy to construct a Landau function which represents the behaviour of the free energy around the critical points. Identifying \bar{r} as the order parameter, this function can be written as

$$\mathcal{W}(\bar{r}, T) = \frac{\omega_3 l^2}{\kappa_5} \left[3\bar{r}^4 - 4\pi l T \bar{r}^3 + (3 - 4\Phi^2) \bar{r}^2 - 24\pi \bar{\alpha} l T \bar{r} + 3\bar{\alpha} \right]. \quad (19)$$

Notice that this expression reduces to the one in [34] when we set $\bar{\alpha}$ to zero and to the one in [1] as we set Φ to zero. It can be checked that at the saddle point of this function, we get the temperature (given by the inverse of the expression in (15)). Substituting back the temperature in \mathcal{W} , we get the free energy W . We have plotted the Landau function in Figure 4. Consider (c) in Figure 4 in particular. This is for $\Phi^2 = 0.2, \bar{\alpha} = 0.01$. Clearly, for $T < T_2$, the global minimum occurs for small \bar{r} , representing a stable small black hole phase. At $T = T_2$, small and big black hole co-exist. At even higher temperature, big black hole represents the stable phase. However, all these phases are meta-stable below $T < T_c$ if we include thermal AdS

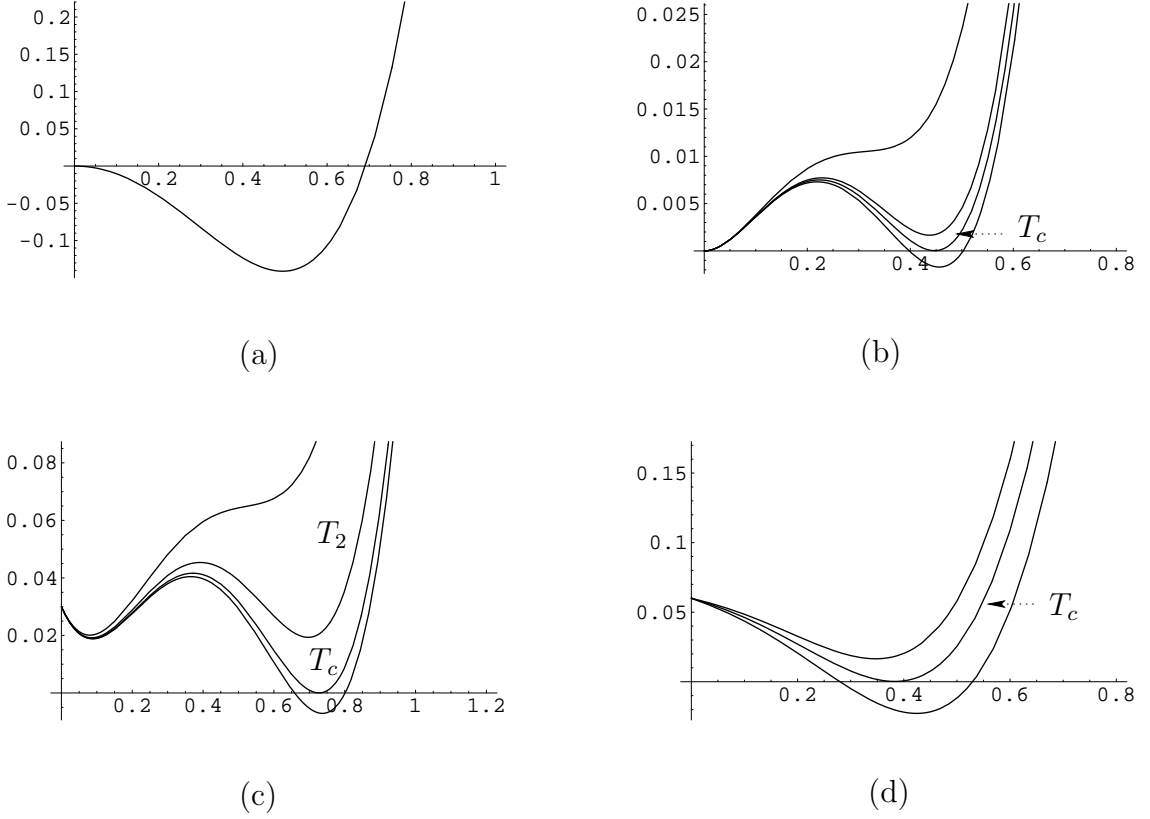


Figure 4: Landau function \mathcal{W} vs. \bar{r} for different temperatures. (a), (b), (c), (d) correspond to values of Φ^2 and $\bar{\alpha}$ of Figure(2)

(representing the horizontal line with $\mathcal{W} = 0$). Big holes then are only stable beyond T_c . Note, that for (a) in Figure 4, black hole is always the stable phase while for (b), there is a crossover from thermal AdS to black hole at T_c . Finally, Figure (d) is similar to (a) except that the $\bar{r} = 0$ hole has more energy than the thermal AdS. To this end, we note that since $W = E - TS - \Phi Q$, we get the energy, entropy and charge as

$$\begin{aligned}
E &= \left(\frac{\partial I_{\text{gc}}}{\partial \beta}\right)_{\Phi} - \frac{\Phi}{\beta} \left(\frac{\partial I_{\text{gc}}}{\partial \Phi}\right)_{\beta} = M \\
S &= \beta \left(\frac{\partial I_{\text{gc}}}{\partial \beta}\right)_{\Phi} - I_{\text{gc}} = \frac{4\pi l^3 \omega_3 \bar{r} (\bar{r}^2 + 6\bar{\alpha})}{\kappa_5} \\
Q &= -\frac{1}{\beta} \left(\frac{\partial I_{\text{gc}}}{\partial \Phi}\right)_{\beta},
\end{aligned} \tag{20}$$

where expressions for Q, M in terms of q, m respectively were defined earlier. It can

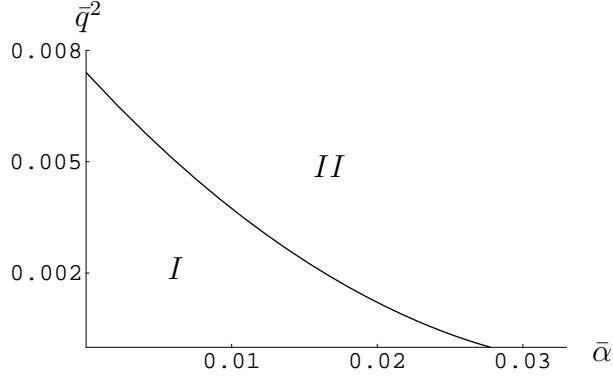


Figure 5: The curve in $\bar{\alpha} - \bar{q}^2$ plane separating regions with various number of solutions.

be checked that the first law of thermodynamics $dE = TdS + \Phi dQ$ is satisfied.

2.2 Canonical ensemble

We now consider the system in canonical ensemble where the charge q is kept fixed. We first note from the expression of the temperature (11) that T is non-negative if

$$\bar{r}^2 + 2\bar{r}^4 - \frac{\bar{q}^2}{\bar{r}^2} \geq 0. \quad (21)$$

When the equality is saturated, the temperature is zero and we call this an extremal black hole. Denoting mass and the scaled horizon radius as \bar{m}_e and \bar{r}_e respectively, we see that the following relation is satisfied:

$$\bar{m}_e = \bar{\alpha} + \frac{\bar{r}_e^2}{2} + \frac{3\bar{q}^2}{2\bar{r}_e^2}. \quad (22)$$

Like in the previous case of fixed potential, we now identify the relevant regions in the $(\bar{\alpha}-\bar{q}^2)$ plane. The curve separating the regions for various number of positive solutions for \bar{r} is given by the following parametric equations in \bar{r} :

$$\begin{aligned} \bar{q}^2 &= \frac{1}{15} (6\bar{r}^6 - \bar{r}^4), \\ \bar{\alpha} &= \frac{5}{3} \left(\frac{\bar{r}^2 - 3\bar{r}^4}{18\bar{r}^2 + 2} \right). \end{aligned} \quad (23)$$

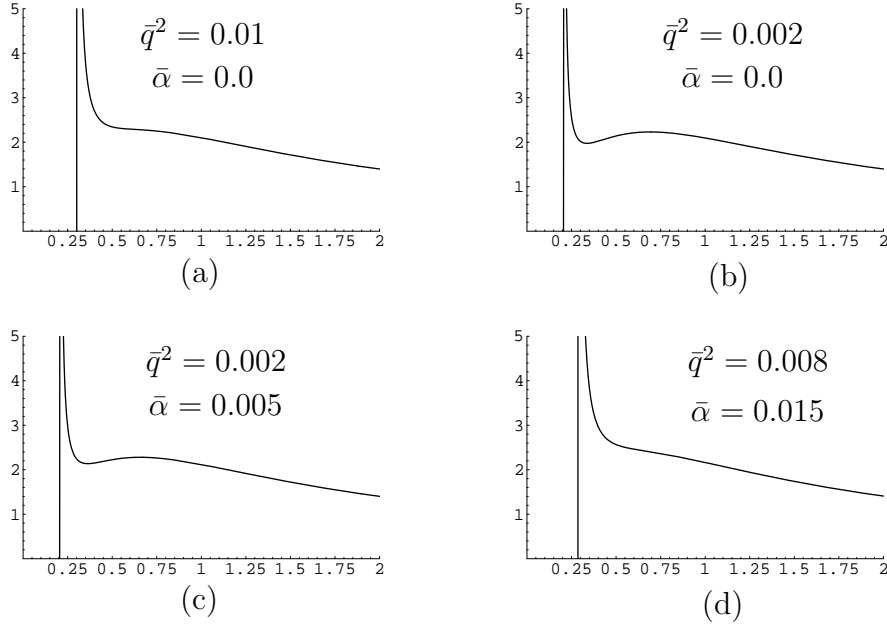


Figure 6: Plots of β vs \bar{r} for various values of $(\bar{q}^2, \bar{\alpha})$.

The curve is shown in Figure 5. It can easily be checked that for any point in region II, there is one real positive root for \bar{r} at any temperature. Below this, that is in region I, there is a maximum of three. Furthermore, unlike the fixed potential case, the vertical \bar{q}^2 -axis i.e. for $\bar{\alpha} = 0$ we also have a maximum of three real positive solutions as long as $\bar{q}^2 < \bar{q}_c^2 (= 1/135)$. We also notice that thermal AdS exists only when $\bar{q}^2 = 0$. The corresponding β - \bar{r} plots for these regions are shown in Figure 6.

Free Energy: We now compute the action (1) in the fixed charge ensemble. After properly adding a boundary charge and subtracting the contribution to the extremal background, we get

$$I_c = \frac{\omega_3 l^2 \beta}{\kappa_5} \left[\bar{r}^2 - \bar{r}^4 + \frac{5\bar{q}^2}{\bar{r}^2} + \frac{8\bar{\alpha}(\bar{q}^2 - \bar{r}^4 - 2\bar{r}^6)}{\bar{r}^2(\bar{r}^2 + 2\bar{\alpha})} - \frac{3}{2}\bar{r}_e^2 - \frac{9\bar{q}^2}{2\bar{r}_e^2} \right], \quad (24)$$

where β is

$$\beta = \frac{2\pi l(\bar{r}^2 + 2\bar{\alpha})\bar{r}}{\bar{r}^2 + 2\bar{r}^4 - \bar{q}^2/\bar{r}^2}. \quad (25)$$

The free energy can therefore be obtained as $F = I_c/\beta$. Behaviours of free energy for different values of $(q^2, \bar{\alpha})$ are shown in Figure 7. We first of all note that, in fixed charge ensemble, black holes with negative free energies are always the stable

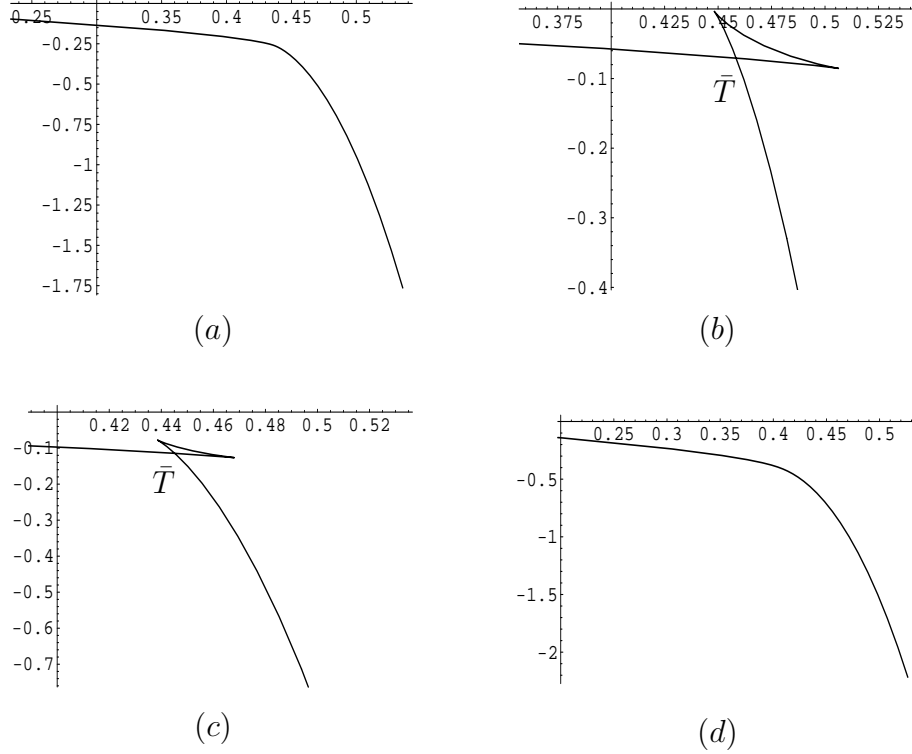


Figure 7: The free energy in canonical ensemble as a function of temperature. (a), (b), (c), (d) represent plots for values of \bar{q}^2 and $\bar{\alpha}$ of Figure (5).

compared to thermal AdS. Secondly, in (a) and (d), we see that given any temperature, there is a single black hole phase, while in (b) and (c), there can at most be three phases. We call them small, big and intermediate black hole phases. We find that at a certain temperature, which we call \bar{T} later, there is a first order phase transition from small to big black hole phase. On the other hand, the intermediate black hole is an unstable phase with negative specific heat. It can be shown by comparing (b) and (c), that \bar{T} decreases as $\bar{\alpha}$ increases.

Finally, the Landau function can be constructed as before. It is given by

$$\mathcal{F}(\bar{r}, T) = \frac{\omega_3 l^2}{\kappa_5} \left[3\bar{r}^4 - 4\pi l T \bar{r}^3 + 3\bar{r}^2 - 24\pi l \bar{\alpha} T \bar{r} + \frac{3\bar{q}^2}{\bar{r}^2} - \frac{9\bar{q}^2}{2\bar{r}_e^2} - \frac{3\bar{r}_e^2}{2} \right]. \quad (26)$$

It can be checked that, at the saddle point, it reproduces correct temperature T and the free energy F . A plot of this function for different temperatures is shown in Figure 8. As can be seen in (a), for high \bar{q} , there is a single black hole phase for

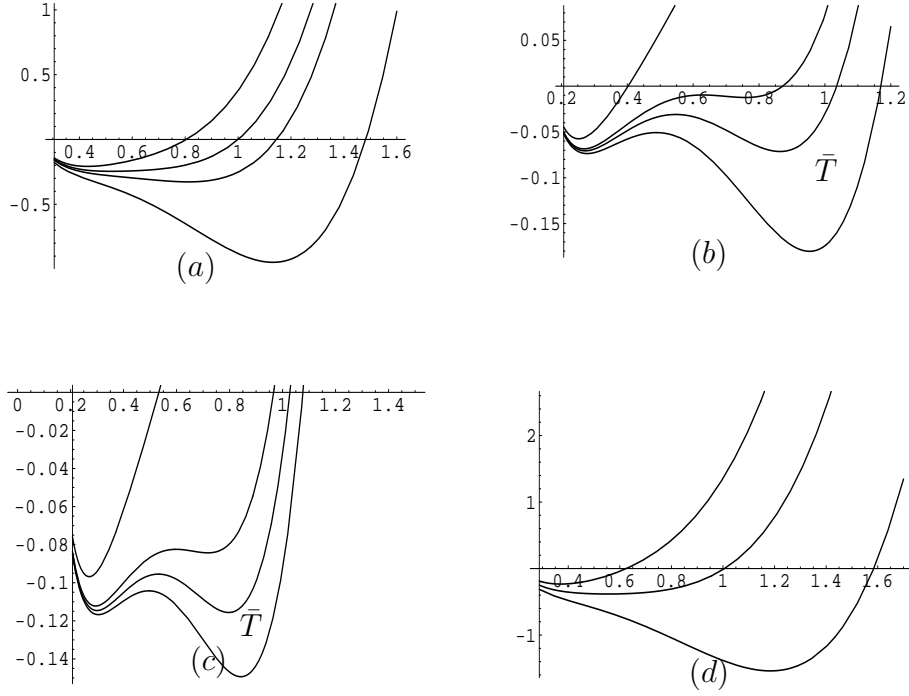


Figure 8: The Landau Function \mathcal{F} as a function of \bar{r} for different temperatures. The critical temperature at which there is a transition between the small black hole to the large black hole is shown by \bar{T} in the figures. Finally, (a), (b), (c), (d) represent plots for values of \bar{q}^2 and $\bar{\alpha}$ of Figure 6.

all temperatures. As we reduce \bar{q} beyond certain value, two new black hole phases appear in (b) for a certain range of temperature. Above and below this range there is only one black hole solution. When the temperature is within this range, for $T < \bar{T}$, the small black hole is favoured. Otherwise, big black hole is the stable one. There are degenerate minima at $T = \bar{T}$ representing phase co-existence.

Now as we turn on $\bar{\alpha}$, we get (c) for low values of $\bar{q}, \bar{\alpha}$. This is similar to (b) except that the critical temperature \bar{T} reduces with $\bar{\alpha}$. Again, for large $\bar{\alpha}$, we get (d) which is qualitatively similar to that of (a).

Finally, since $F = E - TS$, we have

$$E = \left(\frac{\partial I_c}{\partial \beta} \right)_Q = M - M_e$$

$$S = \beta \left(\frac{\partial I_c}{\partial \beta} \right)_Q - I_c = \frac{4\pi l^3 \omega_3 \bar{r} (\bar{r}^2 + 6\bar{\alpha})}{\kappa_5}$$

$$\Phi = \frac{1}{\beta} \left(\frac{\partial I_c}{\partial Q} \right)_\beta = \sqrt{\frac{3}{4}} \left(\frac{\bar{q}}{\bar{r}^2} - \frac{\bar{q}}{\bar{r}_e^2} \right). \quad (27)$$

It can be checked that they satisfy the first law of thermodynamics $dE = TdS + (\Phi - \Phi_e)dQ$.

3 Dual Matrix Model

Classical Type IIB supergravity is dual to $\mathcal{N} = 4$ $SU(N)$ gauge theory at strong coupling. The phases of the gauge theory in this regime of the coupling is very hard to analyze. Assuming the AdS/CFT correspondence to be true one can on the other hand get some understanding from the supergravity computations, that are more tractable. Following these lines, Witten has argued in [4] that the Hawking-Page transition in gravity corresponds to the confinement/deconfinement transition on the boundary. This is the philosophy that we will follow.

In this section, using the AdS/CFT correspondence we write down the dual matrix model corresponding to the R -charged black holes that were studied in the earlier sections. The matrix model is constructed phenomenologically so that it captures the phases of the black holes. The results from the weak coupling computations available in the literature will be used as a guideline in this prescription as was also followed in [1]. We begin with a brief review of some of the results that we will need for the finite temperature gauge theory at weak coupling.

3.1 Weak coupling

$\mathcal{N} = 4$, $SU(N)$ gauge theory at zero and weak couplings has been analyzed by various authors (see for example [6, 7]). For large N , when the t'Hooft coupling $\lambda = g_{YM}^2 N$ is small or zero, some of the results are explicitly known. Specifically, when $\lambda = 0$, it was shown that the boundary gauge theory at finite temperature on $S^3 \times S^1$ undergoes a phase transition that can be identified as the “deconfinement” transition. $S^3 \times S^1$ is a compact manifold and thus allows only colour singlet states by the Gauss law constraint. Though non singlet states are never possible, there are various indications that this transition mimics the deconfinement transition in gauge theories. One of the indications is that there is a jump of the free energy from order N^0 to order N^2 while another is a discrete change in expectation value of the Polyakov loop.

Dimensional reduction of the $\mathcal{N} = 4$ theory on $S^3 \times S^1$ leaves only one massless mode, namely, the zero mode of A_0 . One can thus write down an effective action

by integrating out all massive modes. The resulting model with the gauge fixing conditions, $\partial_i A_i = 0$ and $\partial_t \alpha = 0$, is a zero dimensional matrix model given by,

$$\begin{aligned} Z &= \int DU e^{S_{eff}(U)}, \\ U &= e^{i\beta\alpha} \ , \ \alpha = 1/\omega_3 \int_{S^3} A_0, \end{aligned} \tag{28}$$

where ω_3 denotes the volume of S^3 . Apart from the free energy, whose N dependence reflects the phase of the gauge theory, one can also define a Polyakov loop that acts as an order parameter for the deconfinement transition. The Polyakov loop defined along the time circle of $S^3 \times S^1$ is $(1/N)\text{Tr} P \exp(i \int_0^\beta dt A_0)$, which is nothing but $(1/N)\text{Tr}(U)$ as can be seen from (28). It can be shown that the expectation value of the Polyakov loop does indeed vanish at low temperatures and picks up a non-zero value above some finite temperature, T_H which may be called the Hagedorn or the "deconfinement" transition temperature.

The explicit form of the partition function is given by,

$$\begin{aligned} Z &= \int dU \exp \left[\sum_{n=1}^{\infty} \frac{1}{n} z(x^n) \left(\text{Tr}(U^n) \text{Tr}(U^{-n}) \right) \right] \\ z(x^n) &= z_V(x^n) + z_S(x^n) + (-1)^{n+1} z_F(x^n) \ ; \ x = e^{-\beta}. \end{aligned} \tag{29}$$

Introducing the density of eigenvalues for U and defining $\rho = (1/N)\text{Tr}(U)$ one can write down the effective action as S_{eff} (see [7] for details). In the large N approximation, the various phases are given by the solutions of the saddle point equations of motion. In terms of the density of eigenvalues, the above transition is reflected by a jump of ρ from zero to a nonzero value below and above T_H respectively, where T_H is given by $z(x) = 1$.

These features are some what modified when a small value of the coupling λ is turned on. It is possible to write S_{eff} only in terms of powers of $\text{Tr}(U)$ by using the saddle point equations. An effective action containing only the quartic interactions may be written as ⁹,

⁹This model is obtained by keeping terms upto $\mathcal{O}(\lambda^2)$ in the effective action. In the large N limit such terms come from three loop computations. It also determines the sign of b . In [7] the phases for both the signs of b have been studied. An explicit computation for pure Yang Mills theory on a three sphere at finite temperature shows that b is positive, implying that the transition is of first order at weak coupling [35].

$$Z(\lambda, T) = \int dU \exp \left[a(\lambda, T) \text{Tr}(U) \text{Tr}(U)^\dagger + \frac{b}{N^2}(\lambda, T) \left(\text{Tr}(U) \text{Tr}(U)^\dagger \right)^2 \right]. \quad (30)$$

The equations of motion resulting from (30) are,

$$\begin{aligned} a\rho + 2b\rho^3 &= \rho & 0 \leq \rho \leq \frac{1}{2} \\ &= \frac{1}{4(1-\rho)} & \frac{1}{2} \leq \rho \leq 1. \end{aligned} \quad (31)$$

The matrix model (30) undergoes two different phase transitions as a function of temperature. One is a first order transition like the zero coupling case, when $b > 0$. The other is a third order transition for which the eigenvalue distribution goes from the gapless phase for $0 \leq \rho \leq \frac{1}{2}$, to a phase with a gap for $\frac{1}{2} \leq \rho \leq 1$.

3.2 Strong coupling and comparison to gravity

If one assumes validity of (30) in the strong coupling regime (where a and b are some complicated functions of λ) one may hope to map these phases to those of gravity obtained in the supergravity approximation. It was shown that this simplified model indeed possesses the thermodynamic behaviour expected from gravity when $a < 1$ and $b > 0$ [11]. A new feature that is not visible in the supergravity approximation is the transition corresponding to the third order transition that was mentioned in the earlier paragraph. It was conjectured that this should correspond to black hole string transition [33]. It should however be noted that the matching is only qualitative and the validity of the effective action (30) in the strong coupling regime is only limited to the regions around the critical points.

The phase structure gets modified once we include (α') corrections. In addition to the large stable black hole, there is also a small stable black hole solution along with an intermediate unstable one. There are two phase transitions: (i) From the small to the large black hole (HP1) at T_2 (ii) Between thermal AdS and the large black hole (HP2) at T_c .

In [1] we studied the matrix model that captures these phases in gravity. Since the size of the small black hole is less than $\sqrt{\alpha'}$ while we include corrections only up to first order of α' we discussed both the following possibilities. If we do not trust this solution, the situation is same as that of the case without higher derivative corrections and the (a, b) model (30) itself serves as the dual of gravity. With the α'

corrections in the bulk it is also possible to see the variations of a and b as a function of $1/\sqrt{\lambda}$. An interesting point is to note that b decreases as we decrease λ .

On the other hand, if we trust this solution the minimal action for the matrix model gets modified so that it can reproduce all the features of gravity near the critical points, including the small black hole. This modified action is given by,

$$S(\rho^2) = 2N^2 \left[A_4 \rho^8 - A_3 \rho^6 + A_2 \rho^4 + \left(\frac{1 - 2A_1}{2} \right) \rho^2 \right]. \quad (32)$$

The A_i 's are functions of λ and T . The (a, b) model is recovered when A_3 and A_4 vanishes. The addition of α' corrections in gravity requires higher powers of ρ to be added. In order that the model (32) reproduces all the features of gravity one also needs to restrict the values of A_i 's within certain regions. There is however one saddle point solution that does not have a counterpart in supergravity. This solution is locally unstable and can possibly serve as some stringy decay mode for the small black hole. In the following parts of this section we will use (32) so that it incorporates the phases of charged black holes as discussed in section (2).

3.3 Matrix model with chemical potential

Once we turn on a non-zero chemical potential the coefficients of the matrix models described above will depend on the chemical potential. At zero coupling, *i.e* at $\lambda = 0$, this dependence is easy to determine. The partition function in this case is given by (29) with $z(x^n)$ modified as,

$$z(x^n) = z_V(x^n) + z_S(x^n) \cosh(\mu) + (-1)^{n+1} z_F(x^n) \cosh(\mu/2). \quad (33)$$

This matrix model was studied in [28, 29] and similar to the case of $\mu = 0$, there is first order deconfinement transition at temperature T_H . Where T_H is given by $z(x) = 1$. There is a discontinuous change in ρ from zero to a nonzero value. Above T_H the deconfined phase is preferred and has free energy $\mathcal{O}(N^2)$. Below T_H the preferred confined phase has free energy $\mathcal{O}(1)$.

When a small λ is turned on, to the quadratic order in λ one gets a term of the form $(\text{Tr}(U)\text{Tr}(U^{-1}))^2$. One may thus be inclined to propose a matrix model corresponding to the black holes with chemical potential as was done earlier with the (a, b) model for the black holes zero chemical potential. However, the dependence of the coefficients, (a, b) on the chemical potential, though obvious in the $\lambda = 0$ case, is not easy to determine when $\lambda \neq 0$. As was mentioned, the lowest correction is $\mathcal{O}(\lambda^2)$

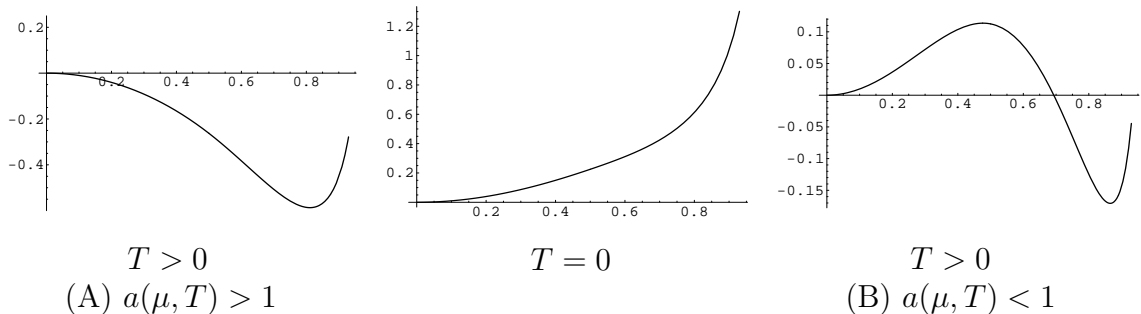


Figure 9: Plots of the matrix model potential *vs.* ρ above μ_c showing the two possible situations at finite temperature. At $T = 0$ the extremal black hole decays into AdS, shown as a saddle point at $\rho = 0$.

that involves a three loop computation¹⁰. On the other hand, an alternative approach is to write down a model in the strong coupling regime by comparing with gravity. Though we do not hope to determine the exact dependence of the parameters on the chemical potential, the restrictions on them so that the matrix model reproduces the qualitative features of gravity can be inferred.

Let us begin with the case without α' corrections. We will consider the equation (31), where now apart from λ and T , a and b are also functions of the chemical potential μ .

When comparing with gravity, $a(\lambda, T, \mu)$ and $b(\lambda, T, \mu)$ will be assumed to be positive for all values of μ . We have seen in section (2.1) that there exists a critical value of the potential (μ_c) above which there is only one solution. Below this there are a maximum of two solutions. The phase structure below the critical potential is same as that of the uncharged case. This is reproduced by the (a, b) model when $a < 1$ and $b > 0$ as described in [11].

From equation (15), we see that the radius of the small black hole at and above the critical potential, becomes zero and negative respectively. The black hole with positive radius approaches an extremal limit at $T = 0$. We know that thermal AdS exists for all temperatures and at $T = 0$ the gauge theory is in the confined phase. We thus have two solutions in gravity corresponding to the confined phase. However the extremal black hole being nonsupersymmetric will ultimately decay into AdS at zero temperature [25, 26]. We do not expect to capture the dynamics of this decay with the

¹⁰To our knowledge this computation is not available in the literature. We hope to return to this problem in future.

static potential given by the (a, b) model. In fact the zero temperature configuration with only the AdS is not continuously connected to the finite temperature (a, b) model as we will see below.

At finite temperature, we always need to introduce an unstable saddle point (a maximum). This follows from the observation that the smooth potential given by the (a, b) model which gives two minima (corresponding to thermal AdS and the large black hole in gravity) always includes a maximum in between. For $\mu > \mu_c$ this maximum corresponding to the unstable black hole ceases to show up in gravity above. In the matrix model, we interpret this phenomenon as follows. As μ increases beyond μ_c this unstable saddle point in the matrix model enters the $\rho < 1/2$ region from $\rho > 1/2$ region. Thus the region beyond μ_c corresponds to the values of a and b when the unstable small black hole of the (a, b) model has already undergone the third order Gross-Witten transition [31, 32]. This imposes a constraint on the values of a and b . Another constraint comes from the fact that the energy of the large black hole in this region is lower than thermal AdS for all temperatures. At any finite temperature, the theory is thus always in the deconfined phase. Both of these constraints are satisfied if we set $b > 2(1 - a)$. However, in light of these remarks, it is not possible to tell whether the unstable saddle point has energy less or more than that of AdS or whether it is at $\rho = 0$ or away from it. Thus it gives rise to two possible scenarios depending on whether the unstable saddle point is at $\rho = 0$ or in the region $0 < \rho < 1/2$ as shown in Figure 9. In the following we discuss these two scenarios separately .

(A) Unstable maximum is at $\rho = 0$ ($a(\mu \geq \mu_c, T) \geq 1$): In this case we define the critical potential μ_c by $a(\mu_c, T) = 1$. Here the unstable saddle point at $\rho = 0$ does not correspond to thermal AdS but to the unstable configuration not visible in gravity as mentioned above. Thermal AdS does not feature in the plot. It has energy higher than the black hole. The condition $b > 2(1 - a)$ is automatically satisfied as b is assumed to be positive.

(B) Unstable maximum is at $0 < \rho < 1/2$ ($a(\mu \geq \mu_c, T) < 1$): In this case the saddle point at $\rho = 0$ is thermal AdS. The unstable saddle point has energy higher than AdS. Since the black hole has energy less than AdS, a and b correspond to values above the Hawking-Page transition. Also the saddle point for the maximum is at $\rho < 1/2$. The critical potential in this case is given by, $b(\lambda, T, \mu_c) = 2[1 - a(\lambda, T, \mu_c)]$ or by the curve in the parameter space of a and b that gives the Hawking-Page tran-

sition, depending on whichever satisfies both the above conditions.

At this point we recall the plot of [11] showing the various regions in the $(a - b)$ parameter space. This is shown in Figure 10. For $\mu > \mu_c$ we have the following situation: At $T = 0$ the only solution which is thermal AdS, is given by the region below line I. At any finite temperature the parameters jump to values in regions (A) or (B).

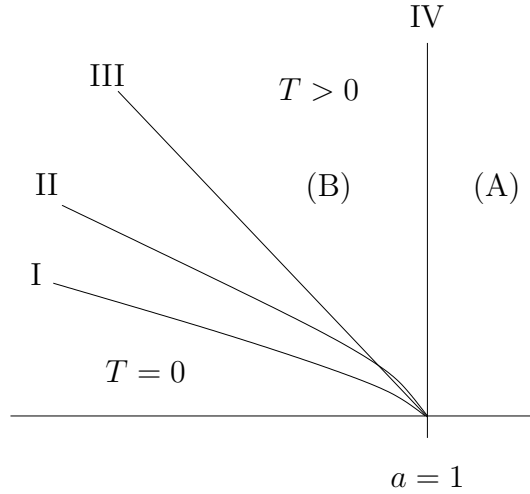


Figure 10: The $a - b$ parameter space for $\mu > \mu_c$. The zero temperature region is below I and the finite temperature region is beyond III or II. Below I there is only one saddle point at $\rho = 0$ corresponding to thermal AdS. On II the Hawking Page transition occurs. III is the Gross-Witten transition line. IV is the line, $a = 1$

The matrix model for the fixed charge is obtained by integrating over the chemical potential. For this we need to know the exact dependence of a and b on μ in this strong coupling regime which we do not have. We note that the possibility (A) incorporates a condition only on a . The condition on b ($b > 2(1 - a)$) is always satisfied in that range of a . This implies that we can consistently assume b to be independent of μ . However the possibility (B) implies that both a and b should be dependent on μ .

Equation(33) shows the exact dependence of a on μ in the free theory. In this case, including only the charged scalars, $a(\lambda, T, \mu) = [c(\lambda, T) + d(\lambda, T) \cos(\mu)]$. If we assume this to hold in the strong coupling regime with b independent of μ one can derive a model for the canonical (fixed charge) ensemble. This will thus be consistent with (A). This fixed charge model was studied in [36]. We will discuss the matrix model

corresponding to the Gauss-Bonnet black holes with fixed charge in section (3.5). Before this in the next section we study the model with fixed potential including α' corrections.

3.4 Including α' corrections : Fixed potential

As mentioned before, once we include α' corrections along with nonzero chemical potential, the coefficients in the action (32) depend also on α' . The equations of motion are of the same form as given in the $\mu = 0$ case:

$$\begin{aligned}\rho F(\rho) &= \rho \quad , \quad 0 \leq \rho \leq \frac{1}{2}, \\ &= \frac{1}{4(1-\rho)} \quad , \quad \frac{1}{2} \leq \rho \leq 1,\end{aligned}\tag{34}$$

where we have defined

$$F(\rho) = \frac{\partial S(\rho^2)}{\partial \rho^2} = N^2[8A_4\rho^6 - 6A_3\rho^4 + 4A_2\rho^2 + (1 - 2A_1)].\tag{35}$$

The potentials that follows from the above action are given by

$$\begin{aligned}V(\rho) &= -A_4\rho^8 + A_3\rho^6 - A_2\rho^4 + A_1\rho^2 \quad , \quad 0 \leq \rho \leq \frac{1}{2} \\ &= -A_4\rho^8 + A_3\rho^6 - A_2\rho^4 + (A_1 - 1/2)\rho^2 - \frac{1}{4}\log[2(1-\rho)] + \frac{1}{8} \quad , \quad \frac{1}{2} \leq \rho \leq 1.\end{aligned}\tag{36}$$

As seen from (34) $\rho = 0$ is always a solution. The action (32) evaluated at $\rho = 0$ vanishes. For zero chemical potential and $\bar{\alpha}$ this solution corresponds to the thermal AdS on the bulk side [11].

In the analysis of phase structure we saw as the chemical potential Φ and temperature T vary we arrive different regions having different thermodynamic features. Similarly in the matrix model as chemical potential and temperature vary the coefficients of the matrix model action vary as well. Thus if we consider a four dimensional space corresponding to the four coefficients of (32) it is sectioned into various regions which are analogous to the regions in the phase diagram. This is essentially same as what we did graphically in Figure 10 for two coefficients. Analogously, here we will identify different regions in four dimensional space of the coefficients with various ranges of temperature and chemical potential.

Let us begin with the various regions in the $(\Phi^2 - \bar{\alpha})$ plane depending on the number and nature of the solutions, as discussed in subsection (2.1) (see Fig. 1). In particular, there is a line in the $(\Phi^2 - \bar{\alpha})$ -plane that separates region with three solutions and that

with one solution. Let us consider constraints imposed on the coefficients A_i that corresponds to these regions or in other words, regions above and below the critical potential μ_c at fixed λ . For that purpose it is useful to consider the quadratic polynomial in ρ^2 : $f(\rho^2) = (1/\rho)\frac{\partial}{\partial \rho}F(\rho)$. This is given by $f(x) = 48A_4x^2 - 24A_3x + 8A_2$. The zeroes of f determine the non-trivial turning points of F . We will see below that the parameters at $T = 0$ are continuously connected to the finite temperature ones for $\mu < \mu_c$ but they are not so for $\mu > \mu_c$ as we saw in absence of α' correction.

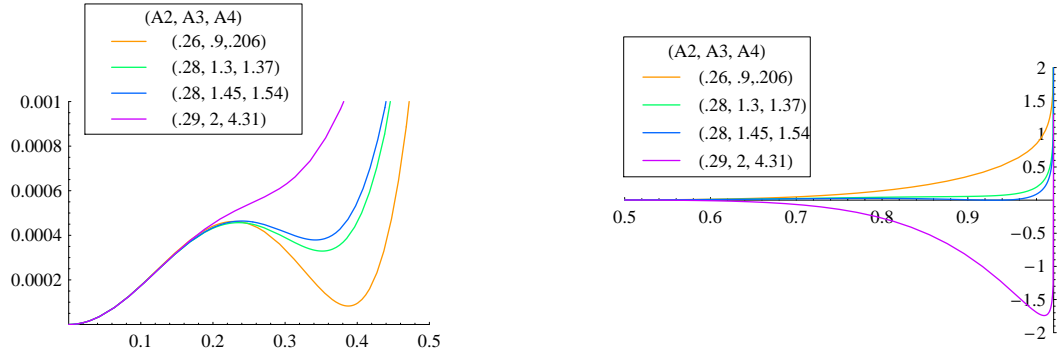


Figure 11: For $\mu < \mu_c$, Potential as function of ρ for the ranges $0 \leq \rho \leq 1/2$ and $1/2 \leq \rho \leq 1$. The values of (A_2, A_3, A_4) used in the plots are given above. $A_1 = 0.02$.

Sub-critical Potential ($\mu < \mu_c$): This corresponds to the region I in Figure 1. In this range the behaviour is very similar to the case of zero chemical potential. As is evident from the plot in Figure 2(c) obtained on the gravity side we have two characteristic temperatures, among others. One is $T = T_{N2}$ where the stable big black hole and unstable intermediate black hole nucleates. Another is $T = T_{N1} > T_{N2}$ where the intermediate unstable black hole combines with stable small black hole and beyond that temperature they cease to exist as solutions. This leads to three qualitatively different ranges of temperature and in the following we discuss them separately.

$T_{N2} < T < T_{N1}$: Here on the gravity side we have three black holes and so we expect at least three solutions of the saddle point equation (34) obtained from the Matrix model. The small black hole has a size of the order of α' . In addition, as we have already seen in the analysis of $\mu = 0$ case [1], we have an (unstable) solution which is a maximum of the potential. Since this solution does not appear in the gravity that is beyond an analysis of order α' . So we expect these two solutions occur generically in the range $0 \leq \rho \leq \frac{1}{2}$. The other two solutions which are analogue of

unstable intermediate black hole and stable big black hole, since they do have bulk analogue we expected them to appear generically in the range $\frac{1}{2} \leq \rho \leq 1$. Therefore we get four solutions for this region. So this region corresponds to the range of the coefficients A_i for which (34) has four solutions within the domain of ρ . From (34) we see this requires $f(\rho^2) = 0$ has two positive solutions $0 \leq \rho_-^2 \leq \rho_+^2 \leq 1$ where ρ_- is a maximum and ρ_+ is a minimum of $F(\rho)$. That $f(\rho^2) = 0$ has two solutions requires

$$\Delta = 3A_3^2 - 8A_2A_4 > 0, \quad A_4 \cdot A_2 > 0, \quad (37)$$

where the second condition is to ensure that both the solutions ρ_\pm^2 are positive. That ρ_\pm are minimum and maximum of F respectively implies $F''(\rho_-) < 0$, $F''(\rho_+) > 0$ from which we obtain

$$\rho_\pm^2 = \frac{A_3}{4A_4} \pm \sqrt{\left(\frac{A_3}{4A_4}\right)^2 - \frac{A_2}{6A_4}}, \quad A_2 > 0. \quad (38)$$

Other conditions that we need to impose so that (34) admits four solutions are $F(\rho_-) > 1$ and $F(\rho_+) < 1$, which when written in terms of A_i 's become

$$\frac{A_2 \cdot A_3}{3A_4} > 2A_1 + 16A_4 \left[\left(\frac{A_3}{4A_4}\right)^2 - \frac{A_2}{6A_4} \right] \rho_-^2, \quad (39)$$

$$\frac{A_2 \cdot A_3}{3A_4} < 2A_1 + 16A_4 \left[\left(\frac{A_3}{4A_4}\right)^2 - \frac{A_2}{6A_4} \right] \rho_+^2. \quad (40)$$

The above conditions (37,38,39, 40) ensure that there exist a minimum (ρ_{min}) corresponding to the small black hole and a maximum (ρ_{max}) that does not have a gravity analogue. These solutions are in general different from ρ_\pm and since F is a cubic polynomial in ρ^2 the expressions are complicated. In addition, on the gravity side we saw that stable small black hole have positive energy. So we expect the solution of the saddle point equation that correspond to this stable small black hole should have positive energy. So we need at the minimum

$$V_1(\rho_{min}) > 0. \quad (41)$$

whose explicit form is not very illuminating.

In addition as we said from gravity analysis we expect two solutions should appear, generically, in the first half of the domain of ρ while two other in the second half. We consider two halves of the domain of ρ separately. Let us begin with the range $0 \leq \rho \leq \frac{1}{2}$. That we have two solutions of the saddle point equation (34) in this range imposes two further conditions:

$$\rho_- < \frac{1}{2}, \quad F\left(\frac{1}{2}\right) < 1. \quad (42)$$

(In this form it is easier to obtain the restriction on the parameters. Otherwise we could write $0 < \rho_{min}, \rho_{max} < \frac{1}{2}$ which are more direct but the expressions are cumbersome.) These conditions, when written in terms of the parameters, reduce to the following two equations:

$$\frac{A_3}{4A_4} - \sqrt{\left(\frac{A_3}{4A_4}\right)^2 - \frac{A_2}{6A_4}} < \frac{1}{4} \quad , \quad (43)$$

$$2A_1 + \frac{3A_3}{8} > A_2 + \frac{A_4}{8}. \quad (44)$$

These conditions (37,38,39,40,41) are real inequalities in four parameters. Each of them will give rise to one (or more) codimension 1 wall(s) in the four dimensional parameter space described by A_1, A_2, A_3, A_4 . Since this involves four parameters it is difficult to have a graphical representation of it. As we see each of the inequalities corresponds to wall(s) which we cross when we go beyond this range of temperature and chemical potential. However, crossing the wall corresponding to (41) will take us to some unphysical region as that implies the stable small black hole has energy less than that of AdS which implies on the gauge theory side absence of confinement in low temperature. The equations (43 and 44) also give rise to codimension one walls but a more elaborate analysis is required to understand the correct significance of them.

We expect the other two solutions to appear in the other half namely $\frac{1}{2} \leq \rho \leq 1$. On this part the situation is pretty much similar to that of (a, b) -model. This requires we have one solution $\frac{1}{2} \leq \rho_1 \leq 1$ such that it satisfies

$$F(\rho_1) = \frac{1}{4\rho_1(1-\rho_1)} \quad , \quad F'(\rho_1) > \frac{1}{4}\left(-\frac{1}{\rho_1^2} + \frac{1}{(1-\rho_1)^2}\right), \quad (45)$$

where this ρ_1 will appear as the analogue of the unstable intermediate black hole solution that we got on the gravity side. Actually, this condition is sufficient to ensure that there is the analogue of stable big black hole too. This condition (45) along with (37,38,39,40) completes the list of necessary and sufficient condition to have four solutions of the saddle point equations. As temperature increases, ρ_1 will decrease. At Gross-Witten temperature [31,32] $T = T_g$ this reaches the lower boundary of this region $\rho = \frac{1}{2}$. At $T = T_g$ the restriction on the parameters can be written as

$$2A_1 + \frac{3A_3}{8} = A_2 + \frac{A_4}{8} \quad , \quad 3A_4 + 8A_2 > 6A_3. \quad (46)$$

This corresponds to a third order phase transition.

$T \leq T_{N2}$: In this range of temperature the conditions that we obtain on the first half of the domain of ρ remain the same. On the second half of the domain the two solutions will merge at $T = T_{N2}$. This implies in the four parameter space we are on the wall that corresponds to (45). The following equations corresponds to T_{N2} :

$$F(\rho) = \frac{1}{4\rho(1-\rho)} \quad , \quad F'(\rho_1) = \frac{1}{4}\left(-\frac{1}{\rho_1^2} + \frac{1}{(1-\rho_1)^2}\right). \quad (47)$$

As temperature decreases the value of $F(\rho)$ will monotonically decreases and there will be no solution in the second half.

$T \geq T_{N1}$: Here we have no solution in the first half of domain of ρ at $T > T_{N1}$. But that can happen in two possible ways and we discuss them in the following. One possibility is the two extrema of $V_1(\rho)$ merge at $T = T_{N1}$ which implies we cross the wall corresponds to (39). In terms of the parameters this means at $T = T_{N1}$

$$\frac{A_2 A_3}{3A_4} = 2A_1 + 16A_4 \left[\left(\frac{A_3}{4A_4} \right)^2 - \frac{A_2}{6A_4} \right] \rho_-^2. \quad (48)$$

This is a consistent possibility that can occur in the matrix model. Another significance of this equation is this corresponds to the bound beyond which we get the features of (a, b) -model and so this region sits in the same universality class of that of (a, b) -model.

The second possibility is crossing the wall corresponding to (40), where the minimum of V_1 meets the maximum of V_2 . However, In terms of the coefficients, then, at T_{N1} we have

$$\frac{A_2 A_3}{3A_4} = 2A_1 + 16A_4 \left[\left(\frac{A_3}{4A_4} \right)^2 - \frac{A_2}{6A_4} \right] \rho_+^2. \quad (49)$$

This possibility seems more plausible as it matches with what we saw on the gravity side. There at $T = T_{N1}$ the unstable intermediate black hole merges with the stable small black hole. At this point we should comment on the relative values of T_{N1} and T_g . If $T_{N1} < T_g$ this merging occurs before the system reaches it Gross-Witten point and therefore there will be no Gross-Witten transition. On the other hand for $T_{N1} > T_g$ the intermediate solution has already undergone the GW transition and becomes a black hole of the order of α' . The other possibility is if $T_{N1} = T_g$ where the small black hole merges with the intermediate black hole exactly at the Gross-Witten point or the two walls corresponding to (40) and (43) merge.

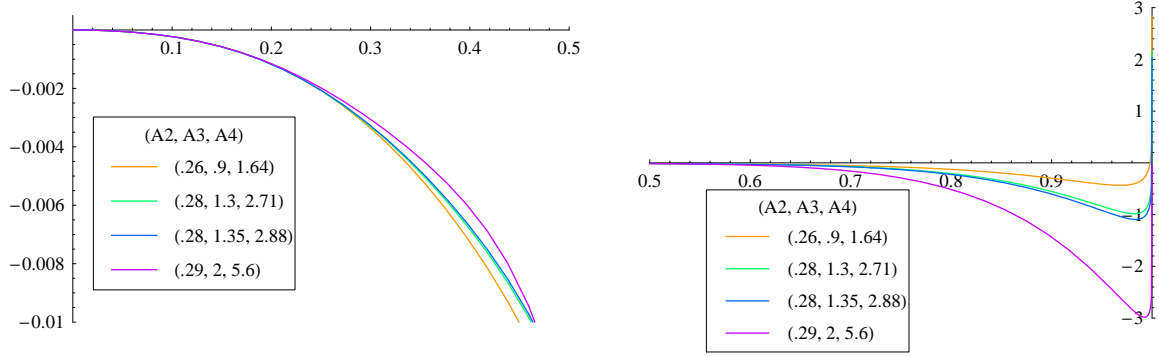


Figure 12: For $\mu > \mu_c$, $A_1 < 0$, $\Delta < 0$: Potential as function of ρ for the range $0 \leq \rho \leq 1/2$ and $1/2 \leq \rho \leq 1$. The values of (A_2, A_3, A_4) used in the plots are given above. $A_1 = -0.02$.

Super-critical Potential ($\mu > \mu_c$): This region corresponds to the parameter space above region I in Figure 1 and therefore should have a single minimum of the potential. In the matrix model like the $\mu < \mu_c$ region here also we have an additional unstable maximum of the potential that does not have any bulk analogue and so it is beyond the gravity analysis of the α' order. Once again we restrict this in the region, $\rho < 1/2$ so that this corresponds to some stringy phase as suggested in [11]. Therefore, similar to the analysis for $\alpha' = 0$ (and unlike the $\mu < \mu_c$ case) we consider two possible scenarios depending on whether the unstable maximum lies at $\rho = 0$ or it lies away from $\rho = 0$. In the following we discuss the two scenarios separately.

(A) Unstable maximum is at $\rho = 0$ ($A_1 < 0$): If we have ($A_1 < 0$) the unstable maximum will always be at $\rho = 0$. In addition, in the matrix model we expect to have one and only one stable minimum for $\rho > 0$ (The energy of this black hole could be greater or less than that of thermal AdS depending on the values of μ and λ (see Figure 3)). The condition $A_1 < 0$ alone does not ensure this and we need to impose additional constraints on A_2 , A_3 and A_4 . We note that there are two ways in which one can ensure that there is only one stable black hole solution. We discuss them separately in the following:

One possibility is, at $\mu = \mu_c$ the three solutions merge into one at some value of $\rho = \rho_+ > 0$. A similar merging occurs on the gravity side when the chemical potential reaches its critical value. Since the corresponding solution is manifested in the gravity limit we expect that $\rho_+ > 1/2$. Then, at $\mu = \mu_c$, apart from the condition $A_1 = 0$,

A_2 , A_3 and A_4 satisfy,

$$V'(\rho_+) = 0 \ ; \ V''(\rho_+) = 0 \ ; \ V'''(\rho_+) = 0 \ \text{for} \ \frac{1}{2} \leq \rho_+ \leq 1. \quad (50)$$

Thus we obtain the parametric solutions of $A_2(\rho_+)$, $A_3(\rho_+)$ and $A_4(\rho_+)$ from (50) which corresponds to the line separating the number of solutions in gravity in Figure 1. We do not write these parametric equations here as they are not compact enough. For, $\rho_+ = 0.8$ we have, $A_1 = 0$, $A_2 = 0.583$, $A_3 = 1.481$, $A_4 = 1.293$.

Examining the equation of motion (34), one can find an indirect way to obtain a (slightly more general) constraint in compact form. This ensures there is exactly one solution at some point $\rho > 0$ in addition to the one at $\rho = 0$. However, that the three solutions merge at this point is not guaranteed. If we relax the first inequality of (37) by making the discriminant Δ negative so that there is no turning point of F then we are left with only a single solution. This can be thought of as crossing the wall corresponds to the first condition of (37) with $\mu = \mu_c$. The merging of the three solutions at this point appears as a special case of it and so that condition is more ramified. We have plotted the associated potentials in Figure 12.

The other possibility that one can consider to obtain a single minimum is setting $A_4(\mu = \mu_c) = 0$ and $A_4(\mu > \mu_c) < 0$. This amounts to relaxing the second inequality of (37) so that one of the turning point becomes imaginary. This corresponds to identifying $\mu = \mu_c$ with the second condition of (37). For this choice, as μ increases beyond its critical value, one of the turning point comes down to $\rho = 0$ and then disappears. This possibility is not continuously connected with the above mentioned constraint, which gives rise to merging of three solutions. However, this possibility can give a simple form for the fixed charge case. We have plotted the related potentials in Figure 13.

(B) Unstable maximum lies at $0 < \rho < 1/2$ ($A_1 > 0$): In this scenario for $\mu > \mu_c$ the unstable maximum is in the range $0 < \rho < 1/2$. The usual saddle point $\rho = 0$ is also there but this time it corresponds to the thermal AdS. In addition, there exists only one minimum. (The energy of this minimum is either greater or less than that of AdS at low temperatures. If the energy is greater than that of AdS energy, at high temperature, the black hole undergoes Hawking Page transition.) In order to make sure that this is the one and the only one minimum, once again we identify μ_c to be the limit where three saddle points merge. However unlike the previous case where the small maximum was at $\rho = 0$, here it lies in $0 < \rho < 1/2$. This configuration

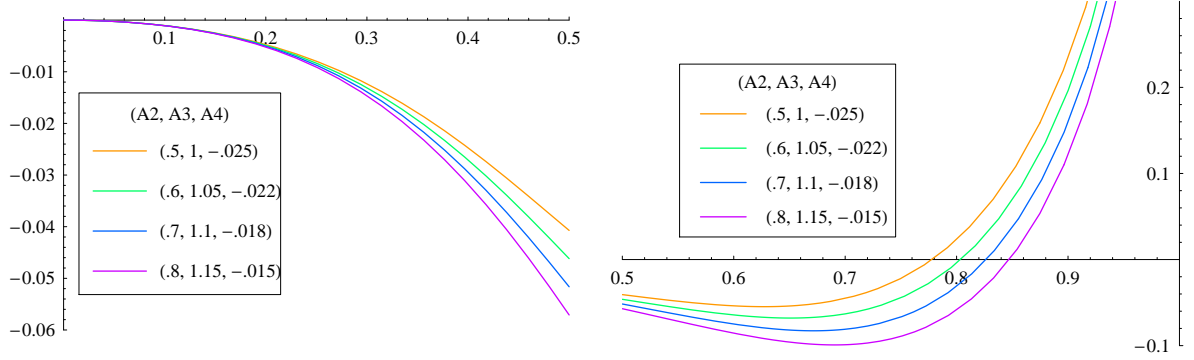


Figure 13: For $\mu > \mu_c$, $A_1 < 0$, $A_4 < 0$: Potential as function of ρ for the range $0 \leq \rho \leq 1/2$. The values of (A_2, A_3, A_4) used in the plots are given above. $A_1 = -0.1$.

satisfies,

$$V'(\rho_+) = 0 ; V''(\rho_+) = 0 ; V'''(\rho_+) = 0 \text{ for } \frac{1}{2} \leq \rho_+ \leq 1. \quad (51)$$

$$\text{and } V'(\rho_-) = 0 \text{ for } 0 \leq \rho_- \leq \frac{1}{2}.$$

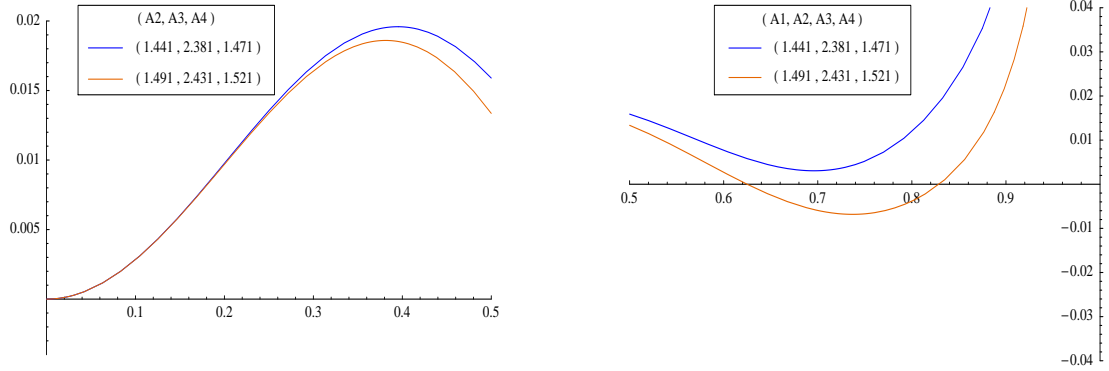


Figure 14: For $\mu > \mu_c$ and $A_1 > 0$: Potential as function of ρ for the range $0 \leq \rho \leq 1/2$ and $1/2 \leq \rho \leq 1$. The values of (A_2, A_3, A_4) used in the plots are given above. $A_1 = 0.298$.

Apart from being functions of ρ_+ the A_i 's are now also functions of ρ_- . With $\rho_- = 0.5$ and $\rho_+ = 0.8$ we get, $A_1 = 0.418$, $A_2 = 1.561$, $A_3 = 2.501$ and $A_4 = 1.691$. In this case the energy of the merging point (ρ_+) is positive. This gives rise to a stable minimum with positive energy as we move beyond μ_c . We now vary the parameters with increasing temperature and see that the minimum crosses zero corresponding to the Hawking-Page transition in the bulk. The plots for $\mu > \mu_c$ are shown in Figure 14.

One can similarly derive the parameters for which the energy of the merging point (ρ_+) is less than zero. This is given by, $\rho_- = 0.4$ and $\rho_+ = 0.72$ which gives $A_1 = 0.006$, $A_2 = 0.06$, $A_3 = 0.291$ and $A_4 = 0.535$. Note that for $\rho_- = 0$ we get ($A_1 = 0$), which is the possibility (A). As we move away from the critical potential, this gives rise to a minimum with energy less than AdS. With further variation of the parameters this saddle point goes deeper as shown in Figure 15. This can be mapped to the variation of the minimum with temperature as it happens for the black hole in gravity.

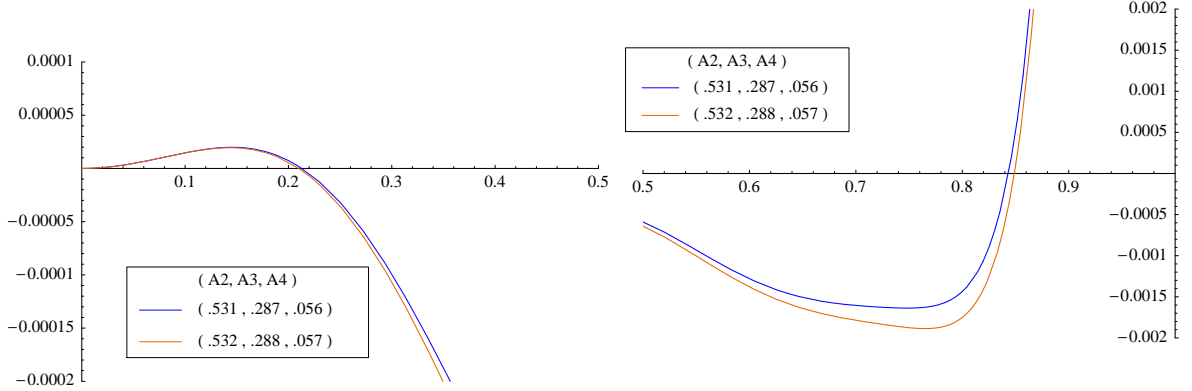


Figure 15: For $\phi > \phi_c$, $A_1 > 0$: Potential as function of ρ for the range $0 \leq \rho \leq 1/2$ and $1/2 \leq \rho \leq 1$. The values of (A_2, A_3, A_4) used in the plots are given above. $A_1 = 0.002$.

In the above discussion we consider, on the matrix model side, the various possibilities, which can reproduce the bulk behaviour that we obtained in the analysis on the gravity side. The different possibilities gives rise to different ranges of the parameters, of which some are mutually exclusive. With this amount of input it is not possible to decide which one is the correct behaviour. We need the explicit dependence of A_i 's on μ in the strong coupling regime. Perhaps a weak coupling calculation of the associated terms in the model can serve as a clue.

3.5 Including α' corrections : Fixed charge

We have seen in the last section that when restricted to various values of the parameters A_i , the matrix model (32) reproduces the features of gravity below and above the critical potential, μ_c . In general thus A_i 's will depend on the chemical potential. In the study of the matrix model for fixed charge, the explicit knowledge of the dependence of A_i 's are necessary. Out of the cases studied in the earlier section, there is

one that allows us to construct a toy model for the fixed charge consistently. This is given by the second possibility of (A), when both A_1 and A_4 become negative above the critical potential.

In the following, we will assume the result from the zero coupling to be valid in this strong coupling regime. In the free theory, A_1 is given by, $(1 - 2A_1) = [c + d \cos(\mu)]$ when matter fields consist of only charged scalars. Since we are only interested in the qualitative features of this model, for simplicity we will take, $A_4 = a_4(\lambda, T) \cos(\mu)$ with A_2 and A_3 functions only of λ and T . The action with this dependence on the potential is,

$$S(\rho^2) = 2N^2 \left[a_4 \cos(\mu) \rho^8 - A_3 \rho^6 + A_2 \rho^4 + \left(\frac{c + d \cos(\mu)}{2} \right) \rho^2 \right]. \quad (52)$$

The partition function for the canonical ensemble is obtained by integrating over the chemical potential. Hence following [36], we write,

$$Z(Q, T, \lambda) = \int d\mu \exp(-i\mu Q) \int d\rho \exp\{-N^2 V(\rho, \mu)\}, \quad (53)$$

where, the potential is,

$$\begin{aligned} V(\rho) &= -\frac{1}{2N^2} S_{eff}(\rho^2) + \frac{1}{2} \rho^2, & 0 \leq \rho \leq \frac{1}{2}, \\ &= -\frac{1}{2N^2} S_{eff}(\rho^2) - \frac{1}{4} \log[2(1 - \rho)] + \frac{1}{8}, & \frac{1}{2} \leq \rho \leq 1, \end{aligned} \quad (54)$$

with,

$$S_{eff}(\rho^2) = N^2 [c\rho^2 + 2A_2\rho^4 - 2A_3\rho^6] + \log [I_Q (N^2(2a_4\rho^8 + d\rho^2))]. \quad (55)$$

Here $I_Q(x)$ is a Bessel Function. We are interested in the large N limit. This is obtained by keeping in mind that $Q^2 \sim \mathcal{O}(N^2)$ so that $Q^2 = N^2 q$ where $q \sim \mathcal{O}(1)$. The resulting effective action in the large N limit is thus,

$$\begin{aligned} S_{eff}(\rho^2) &= N^2 [c\rho^2 + 2A_2\rho^4 - 2A_3\rho^6] + \\ &+ N^2 q \left[\left(1 + \frac{\rho^4(d + 2a_4\rho^6)^2}{q^2} \right)^{\frac{1}{2}} + \log \left[\frac{\frac{\rho^2(d + 2a_4\rho^6)}{q}}{1 + \left\{ 1 + \frac{\rho^4(d + 2a_4\rho^6)^2}{q^2} \right\}^{\frac{1}{2}}} \right] \right] \\ &+ \mathcal{O}\left(\frac{1}{N^2}\right). \end{aligned} \quad (56)$$

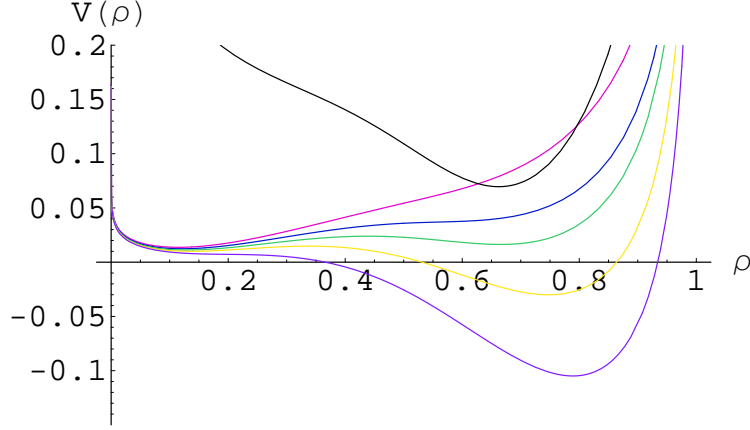


Figure 16: Coloured curves: Potential for various temperatures corresponding to the variations of A_1 , A_2 , A_3 , a , c and a_4 for $q < q_c$ Black curve: Potential for $q > q_c$.

Defining, $F(\rho) = \partial S(\rho^2)/\partial \rho^2$, the equation of motion is given by (34).

The phase structure is qualitatively the same as when there are no α' corrections. Unlike the fixed potential thermal AdS is not a solution. It is easily seen from (56) that $\rho = 0$ is not a solution of the equation of motion. We have seen in section 2.2, that there exists a critical charge for a fixed $\bar{\alpha}$ beyond which there is only one solution. Below this critical charge there are a maximum of three solutions. See equation (23) and Figure 5. In the matrix model, this critical charge (q_c) is given by the merging of the three saddle points of (54).

Figure 16 shows the thermal history for the canonical ensemble. The coloured curves are for $q < q_c$ for some fixed λ . This corresponds to region *I* in Figure 5. At low temperatures, there is a single minimum in the range $0 < \rho < 1/2$ (curves in pink). This corresponds to the small black hole. Two new saddle points appear at $T = T_3$ with the new minimum in the range $1/2 < \rho < 1$ (shown in blue). These correspond to the intermediate (unstable) and large black holes. The small black hole has lower energy upto T_c (the green curve), beyond which the large black hole phase is favoured (yellow). Thus there is a phase transition at T_c corresponding to the one in the bulk. The small and the intermediate black holes disappear at T_1 and at high temperature, the large black hole (the phase with the saddle point in the range $1/2 < \rho < 1$) remains (shown in purple).

The black curve in Figure 16 shows the single saddle point when $q > q_c$. This corresponds to the single large black hole that exists above the critical charge for fixed $\bar{\alpha}$, in the region *II* of Figure 5.

References

- [1] T.K. Dey, S. Mukherji, S. Mukhopadhyay and S. Sarkar, *Phase transitions in higher derivative gravity*, JHEP 04 (2007) 014 [arXiv:hep-th/0609038].
- [2] J. M. Maldacena, *The large N limit of superconformal field theories and supergravity*, Adv. Theor. Math. Phys. **2**, 231 (1998) [Int. J. Theor. Phys. **38**, 1113 (1999)] arXiv:hep-th/9711200.
- [3] E. Witten, *Anti-de Sitter space and holography*, Adv. Theor. Math. Phys. **2**, 253 (1998) [arXiv:hep-th/9802150].
- [4] E. Witten, *Anti-de Sitter Space, Thermal Phase Transition, And Confinement In Gauge Theories*, Adv. Theor. Phys. 2 (1998) 505 [arXiv:hep-th/9803131].
- [5] S. Hawking and D. Page, *Thermodynamics of black holes in anti-de Sitter space*, Commun. Math. Phys. 87 (1983) 577.
- [6] B. Sundborg, *The Hagedorn transition, deconfinement and $N = 4$ SYM theory*, Nucl. Phys. B **573**, 349 (2000) [arXiv:hep-th/9908001].
- [7] O. Aharony, J. Marsano, S. Minwalla, K. Papadodimas and M. Van Raamsdonk, *The Hagedorn/Deconfinement Phase Transition in Weakly Coupled Large N Gauge Theories*, Adv. Theor. Math. Phys. 8 (2004) 603 [arXiv:hep-th/0310285].
- [8] S. Kalyana Rama and B. Sathiapalan, ‘*The Hagedorn transition, deconfinement and the AdS/CFT correspondence*, Mod. Phys. Lett. A **13**, 3137 (1998) [arXiv:hep-th/9810069].
- [9] H. Liu, *Fine structure of Hagedorn transition*, arXiv:hep-th/0408001.
- [10] M. Brigante, G. Festuccia and H. Liu, *Hagedorn divergences and tachyon potential*, arXiv:hep-th/0701205.
- [11] L. Alvarez-Gaume, C. Gomez, H. Liu and S. Wadia, *Finite temperature effective action, AdS_5 black holes, and $1/N$ expansion*, Phys. Rev. D **71** (2005) 124023 [arXiv:hep-th/0502227].
- [12] P. Basu, B. Ezhuthachan and S. R. Wadia, *Plasma balls / kinks as solitons of large N confining gauge theories*, JHEP **0701**, 003 (2007) [arXiv:hep-th/0610257].

- [13] D. G. Boulware and S. Deser, *String Generated Gravity Models*, Phys. Rev. Lett. **55**, 2656 (1985).
- [14] R. C. Myers, *Superstring gravity and black holes*, Nucl. Phys. B **289** (1987) 701.
- [15] S. Nojiri and S. D. Odintsov, Phys. Lett. B **521** (2001) 87 [Erratum-ibid. B **542** (2002) 301] arXiv:hep-th/0109122.
- [16] R. G. Cai, *Gauss-Bonnet black holes in AdS spaces*, Phys. Rev. D **65**, 084014 (2002) [arXiv:hep-th/0109133].
- [17] M. Cvetič, S. Nojiri and S. D. Odintsov, *Black hole thermodynamics and negative entropy in deSitter and anti-deSitter Einstein-Gauss-Bonnet gravity*, Nucl. Phys. B **628**, 295 (2002) [arXiv:hep-th/0112045].
- [18] Y. M. Cho and I. P. Neupane, *Anti-de Sitter black holes, thermal phase transition and holography in higher curvature gravity*, Phys. Rev. D **66**, 024044 (2002) [arXiv:hep-th/0202140].
- [19] I. P. Neupane, *Thermodynamic and gravitational instability on hyperbolic spaces*, Phys. Rev. D **69**, 084011 (2004) [arXiv:hep-th/0302132].
- [20] T. Torii and H. Maeda, *Spacetime structure of static solutions in Gauss-Bonnet gravity: Neutral case*, Phys. Rev. D **71**, 124002 (2005) [arXiv:hep-th/0504127].
- [21] S. S. Gubser, I. R. Klebanov and A. A. Tseytlin, *Coupling constant dependence in the thermodynamics of $N = 4$ supersymmetric Yang-Mills theory*, Nucl. Phys. B **534**, 202 (1998) [arXiv:hep-th/9805156].
- [22] M. Li, *Introduction to M theory*, arXiv:hep-th/9811019
- [23] K. Landsteiner, *String corrections to the Hawking-page phase transition*, Mod. Phys. Lett. A **14**, 379 (1999) [arXiv:hep-th/9901143].
- [24] M. M. Caldarelli and D. Klemm, *M-theory and stringy corrections to anti-de Sitter black holes and conformal field theories*, Nucl. Phys. B **555**, 157 (1999) [arXiv:hep-th/9903078].
- [25] A. Chamblin, R. Emparan, C.V. Johnson and R.C. Myers, *Charged AdS Black Holes and Catastrophic Holography*, Phys. Rev. D **60**, 064018 (1999) [arXiv:hep-th/9902170].

- [26] A. Chamblin, R. Emparan, C.V. Johnson and R.C. Myers, *Holography, Thermodynamics and Fluctuations of Charged AdS Black Holes*, Phys. Rev. D **60**, 104026 (1999) [arXiv:hep-th/9904197].
- [27] T. Torii and H. Maeda, *Spacetime structure of static solutions in Gauss-Bonnet gravity: charged case*, Phys. Rev. D **72** (2005) 064007 [arXiv:hep-th/0504141].
- [28] D. Yamada and L.G. Yaffe, *Phase Diagram of $N=4$ Super-Yang-Mills Theory with R -Symmetry Chemical Potentials*, JHEP 0609:027,2006 [arXiv:hep-th/0602074].
- [29] T. Harmark and M. Orselli, *Quantum mechanical sectors in thermal $N = 4$ super Yang-Mills on $R \times S^3$* , Nucl. Phys. B **757**, 117 (2006) [arXiv:hep-th/0605234].
- [30] L. Alvarez-Gaume, P. Basu, M. Marino and S. R. Wadia, *Blackhole / string transition for the small Schwarzschild blackhole of $AdS_5 \times S^5$ and critical unitary matrix models*, Eur. Phys. J. C **48**, 647 (2006) [arXiv:hep-th/0605041].
- [31] D. J. Gross and E. Witten, *Possible Third Order Phase Transition In The Large N Lattice Gauge Theory*, Phys. Rev. D **21**, 446 (1980).
- [32] S. R. Wadia, *$N = \text{Infinity}$ Phase Transition In A Class Of Exactly Soluble Model Lattice Gauge Theories*, Phys. Lett. B **93**, 403 (1980).
- [33] G. T. Horowitz and J. Polchinski, *A correspondence principle for black holes and strings*, Phys. Rev. D **55**, 6189 (1997) [arXiv:hep-th/9612146].
- [34] A. Biswas and S. Mukherji, *On the Hawking-Page transition and the Cardy-Verlinde formula*, Phys. Lett. B **578**, 425 (2004) [arXiv:hep-th/0310238].
- [35] O. Aharony, J. Marsano, S. Minwalla, K. Papadodimas and M. Van Raamsdonk, *A first order deconfinement transition in large N Yang-Mills theory on a small S^3* , Phys. Rev. D **71** (2005) 125018 [arXiv:hep-th/0502149].
- [36] P. Basu and S.R. Wadia, *R -charged AdS_5 black holes and large N unitary matrix models*, Phys.Rev. D **73** (2006) 045022 [arXiv:hep-th/0506203].